



SEGMENTATION OF IRIS USING DAUGMAN'S ALGORITHM

Patil Ashwini B¹, Dr.Mrs.V.Jayashree²

Abstract—Security is the main concern in majority of the recognition techniques that are used in various Biometric systems. The focus here is to subject the eye image to segmentation process to reduce the redundant data and noise from the image of eye. So this paper represents the segmentation of the eye images to extract the actual iris region from entire eye image. The eye images are taken from the CASIA database (Chinese academy of Sciences). All the iris images were subjected to segmentation process using Canny edge detector for edge detection from which outer and inner boundaries of iris eye images were obtained by Hough transform. This was followed by eyelashes occlusion and normalization by subjecting these images to Daugman's rubber sheet model which then generated the iris templates. From the normalized 280x320 pixel image, redundant data was removed converting the iris image to a size of 50x250 pixels. This procedure was applied on all 756 eye images of 108 persons each with 7 different orientations. The experimentation has shown that, there is a large variation in average value of iris/pupil radius (from 100 to 128.53 pixels) / (38.71 to 45.72) respectively whereas variation in standard deviation value for iris/pupil (from 1.13 to 5.77) / (from 1.25 to 3.4) respectively for the different iris images of 10 people. This is a desired feature of iris segmentation for iris recognition. Thus this segmentation approach has resulted into reduced useful iris information for further classification and iris identification.

Keywords— Canny edge detector, Hough Transform, Daugman's rubber sheet model, Image Normalization

1. INTRODUCTION

There are many biometric systems based on face recognition, finger print recognition, voice recognition, signature recognition, hand geometry and iris recognition. Iris recognition is perhaps the most accurate means of personnel identification due to the uniqueness of the patterns contained in each iris.

The organ which is easily visible from outside of every person's eye is the iris in an eye region. After the eight month of gestation period the annular structure of iris region is completed which does not change further and become a unique structural identity of every individual even the identical twins have different iris structure. The iris region is present between sclera (whitish part of eye) and pupil (blackish part). Arching ligaments, furrows, ridges, crypts, rings, corona, freckles and a zigzag collarets are the unique features present in iris region of every eye and these features cannot be surgically tampered. There are many biometric systems for identification such as face recognition, finger print recognition, voice recognition, signature recognition, hand geometry and iris recognition.

The segmentation of iris plays the crucial role in accuracy of iris recognition. Ghassa Mahmoud Husein Amer [1] et al. implemented different edge detection operators. He concluded that the Canny edge detector gives more accurate results than other operators. Further shape of the inner and outer boundary was found by the Hough transform which is mentioned by author L. Chandrasekhar [2] et al. when he implemented the Hough Transform to compute the parameter of two circles in the determined region thus help to localize actual iris region in of an eye surface. For proper edge analysis there is a need to select the proper scale which requires the smooth image which can be obtained by using Gaussian filter. Daugman J. used the rubber sheet model for normalization procedure to overcome inconsistencies in dimension of circular region to get more accurate normalized binary iris images that helped for iris feature extraction and classification [3]. This method is mostly used over Wildes method [4] as it is less sensitive to some details, also the Daugman's method is easy to implement.

Taking these best approaches into consideration, a robust iris segmentation technique is presented in this paper. Section II describes the theoretical background on iris recognition whereas section III describes the implemented methodology with mathematical analysis. Results and observations are reported in section IV. Conclusion and future scope is explained in section V.

2. THEORETICAL BACKGROUND OF IRIS SEGMENTATION

Edge represents the high frequency component where speckle noises are present so the Canny edge detector is used as it includes the Gaussian smoothing element that smoothen the images significantly. As compared to other edge detection operators used in image processing for edge detection the Canny operator is less affected by spurious noise. The both fast and slow variations in the gray level of image can be detected more efficiently by the Canny operator.

As Hough transform tolerates gaps in the boundary and is unaffected by any noisy region, so it is useful in finding the circular boundaries in an eye image. The circular region of radius r and center (a, b) characteristic equation is given by:

(1)

¹ Electronics Engineering, DKTE Society's Textile & Engineering Institute, Ichalkaranji (An Autonomous Institute), Ichalkaranji, India

² Electronics Engineering, DKTE Society's Textile & Engineering Institute, Ichalkaranji (An Autonomous Institute), Ichalkaranji, India

This two equations further describe the circle region the equations are as follows:

$$x = a + r \cos \theta \quad (2)$$

The Daugman rubber sheet model is used for conversion of Cartesian to polar coordinate system of the eye images which is explained further with mathematical analysis.

3. IMPLEMENTATION STEPS OF SEGEMENTATION OF EYE IMAGES USED IN IRIS RECOGNITION SYSTEM

In recognition technique, image capturing and accuracy in segmentation are the important factors which help to increases the accuracy rate of identification. The process of identification goes through the following process where the iris images used for experimentation are from CASIA database of iris images, then followed by segmentation process which includes steps from 1 to 3, finally step C corresponding to the template generation.

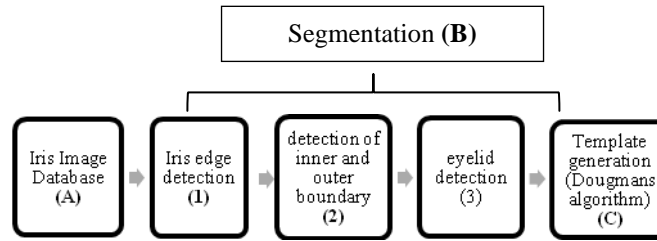


Fig.1. Block diagram

3.1 Iris Image Database

For experimentation a standard CASIA database which contains the gray scale images each with size 280x320 pixels is used. It consists images of eyes of 108 different persons captured with the close proximity and different orientation angle and they are captured digital optical sensor designed by NLPR (National Laboratory for Pattern Recognition- Chinese academy of Sciences) [8]. All the images in this database consists Asian people.

3.2 Segmentation Process of Eye image

Iris segmentation is the process were iris region is been isolated from the eye image and it approximated by the two boundaries that are inner (pupil) and outer (sclera) and iris region present in between the two boundaries. A unique process is required to isolate the iris region and exclude the remaining region. Segmentation process includes following stages Edge detection, finding a circle and Eyelid detection.

3.3 Iris image Edge detection

In segmentation process, to detect the iris boundary, it is necessary to create an edge map which can be accomplished using the canny edge detector. The Canny edge detector first smoothen the image to eliminate noise. It finds the image gradient to highlight regions with high spatial derivatives. In non-maxima suppression the pixel values which don't contain maximum value are suppressed and further the nonmaxima array can be reduced by hysteresis.

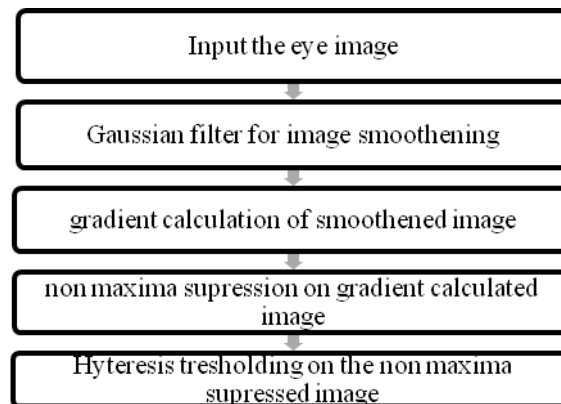


Fig.2. Flow chart canny edge detection

The details in the flow chart are given further.

- Image smoothening (Gaussian filter)

The image smoothing is required firstly to remove the noise present in an eye image at higher frequency due which the eye gets blurred. The smoothing in an image lead the blurring of the image and it can be controlled by σ which is spread the Gaussian. The $I(i,j)$ which denotes the iris image and $G(i,j)$ denotes the Gaussian Smoothing Filter which are . 2-D convolution operator Then convolution of $I[i,j]$ and $G[i,j]$ is given by[B1],

$$S [i,j] = G[i,j]*I[i,j] \tag{3}$$

Where an array of smoothed data is represented by $S [i, j]$.
The 2D form of Gaussian distribution is as below;

$$\tag{4}$$

Where Standard Deviation is denoted by σ .

- Gradient Calculation of image

The large variation in pixel value in eye image is detected by the gradient operator. The large change leads to large value, firstly, the gradient of the smoothed array $s[i,j]$ is used to produce partial derivatives $P[i,j]$ and $Q[i,j]$ respectively, the magnitude and orientation of gradient can be computed as,

$$I[i,j]= \tag{5}$$

$$M[i,j] = \sqrt{P[i,j]^2 + Q[i,j]^2} \tag{6}$$

$$\theta[i,j] = \tan^{-1} (Q[i,j]/P[i,j]) \tag{7}$$

$M[i,j]$ is vector gradient and $\theta[i,j]$ is phase angle.

- Non maxima suppression on gradient calculated eye image

The pixel coordinates whose strength is maximum after gradient calculation in particular direction are considered as the edge points and remaining pixel value whose value less the local maxima point are assigned with zero value.

- Hysteresis Thresholding on non-maxima suppressed image

The nonmaxima suppressed image array is reduced by thresholding. The hysteresis thresholding is used so that lines that include strong and weak gradient are not splitted. This requires two thresholds $T1$ and $T2$.

3.4 Detection of inner & outer boundary of iris using Hough transform

After finding the edge map of input eye image by Canny edge detector, next step is to find radius and center co-ordinates of the outer and inner circular boundary of iris region. The circular Hough transform is employed to find out the radius and center coordinates of the circular boundary of pupil and iris outer boundary. From the edge map cast the votes in Hough space where the parameter of the circle are tracked through each edge point passing on circle. These parameters are the Centre coordinates x and y , and the radius r , which are able to define any circle according to the equation,

$$x^2 + y^2 - r^2 = 0 \tag{8}$$

3.5 Eyelid and eyelashes detection and elimination

The human eye eyelids, eyelashes create problem in recognition system which is redundant data present in an eye image so it necessary to remove this data to make this system more efficient in identification. Using linear Hough transform a line is placed on both eyelid and eyelashes to remove that particular region.

3.6 Template generation using Normalization of segmented image(formation of Template)

To reduce the inconsistent dimension caused by pupil dilation due to variation in illumination levels that leads to stretching in iris, there is a need of normalization process in order to obtain fixed dimension for iris known as template of a segmented image.To convert circular iris to rectangular pattern with fixed size it is required to convert the Cartesian coordinates to polar coordinates [6], [7] and pixels are remapped in localized iris region by using homogeneous rubber sheet model. The pupil dilation, non-concentric pupil displacement and imaging distance are accounted in homogenous rubber sheet model However, rotation variance is not compensated by this algorithm.

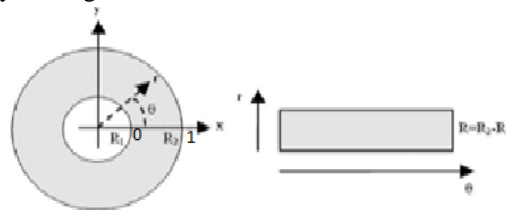


Fig.3.Normalized image after segmentation

For polar to Cartesian transformation the following mathematical equations are used, those are as given below,

$$\theta [0,2 \pi], r[0,1],I(x(r,\theta),y(r,\theta)) \rightarrow I(r,\theta) \tag{9}$$

$$x(r,\theta) = (1-r)x_{pu}(\theta) + rx_i(\theta) \quad (10)$$

$$y(r,\theta) = (1-r)y_{pu}(\theta) + ry_i(\theta) \quad (11)$$

$$x_{pu}(\theta) = x_{pc}(\theta) + rp \cos(\theta) \quad (12)$$

$$y_{pu}(\theta) = y_{pc}(\theta) + rp \sin(\theta) \quad (13)$$

$$x_i(\theta) = x_{ic}(\theta) + ri \cos(\theta) \quad (14)$$

$$y_i(\theta) = y_{ic}(\theta) + ri \sin(\theta) \quad (15)$$

where,

$I(x,y)$ is the iris region, (x,y) , (ρ,θ) , are the Cartesian and polar coordinates respectively (x_{pu},y_{pu}) and (x_i,y_i) are coordinates on pupil and sclera boundaries along the θ direction (x_{pc},y_{pc}) , (x_{ic},y_{ic}) are the coordinates of pupil and iris centres.

4. EXPERIMENTAL PROCEDURE

Steps used in experimentation

1. Iris image is subjected to Segmentation followed by normalization method, where the canny edge detector gives high positioning accuracy
2. In second step the circular Hough transform is used to obtain accurately inner pupil boundary and outer iris boundary
3. In the 3rd step the linear Hough transform is used to detect the top and the bottom eyelids and eyelashes.
4. Next the Daugman's rubber sheet model is used in normalization process on the preprocessed images to convert the result in Cartesian coordinate system into polar coordinate
5. Using step in 4, radius and angles can be plotted in rectangular form.
6. The steps from 1-5 are repeated for all images in CASIA database. In the experimentation 10 images of 7 different orientations of people from are used as benchmark results obtained which are presented in section (V).

5. RESULTS AND DISCUSSION

Here the experimentation is carried on 108 different person eye images with 7 different orientation angles together forming 756 samples of images in the CASIA database. Two original eye image samples of two different person are shown in Figure.4.(a) and (b) respectively.

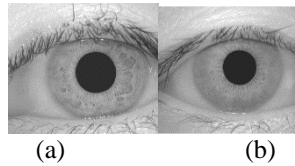


Figure.4. Original Raw Data Of The Eye Images From The CASIA Database

Figure.5. (a) & (b) are obtained by subjecting original eye images of Figure.4. (a) & (b) to gradient calculation.

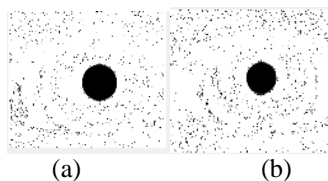


Figure.5. Gradient Calculation On The Eye Images

Image of Figure.5. (a) & (b) are subjected to the contrast enhancement by adjusting the Gamma value and result images so obtained are as shown in the Figure.6. (a) & (b). Further non max value from Figure.6. (a) & (b) are suppressed which gives eye images as in Figure.7. (a) & (b) which are then subjected to the hysteresis thresholding where the outer boundary is obtained as shown in Figure.8. (a) & (b).

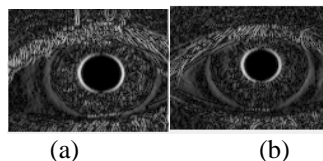


Figure.6. Contrast Enhancement Of Amplitude Images

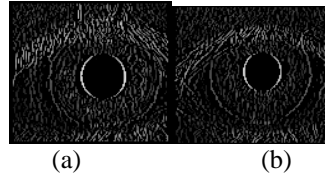


Figure.7. Non Maxima Suppression Of The Images

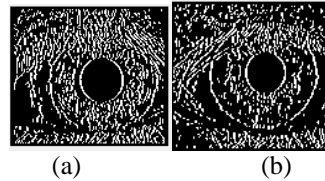


Figure.8. Hysteresis Thresholding On The Images

Results of inner edge detection are shown in Figure 9 to Figure 13. The procedure similar to outer boundary extraction was adopted with only change in the selection of hysteresis thresholding values. Threshold values for both inner and outer boundary extraction are chosen using trial and error method.

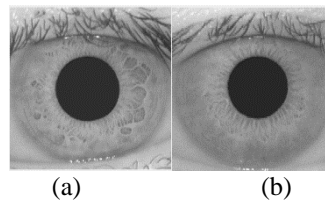


Figure.9. Eye Images For Extraction Of Inner Boundary

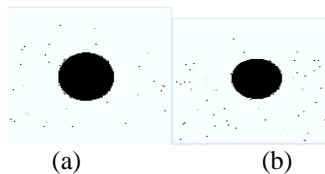


Figure.10. Gradient Amplitude On The Pupil Images

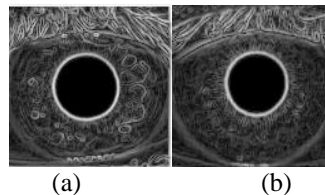


Figure.11. Contrast Enhancement Of Amplitude Images Of Pupil

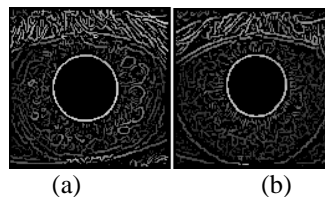


Figure.12. Non Maxima Suppressed On Pupil Of Eye Images

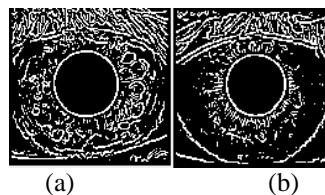


Figure.13. Hysteresis Thresholding On The Pupil Of The Eye Images

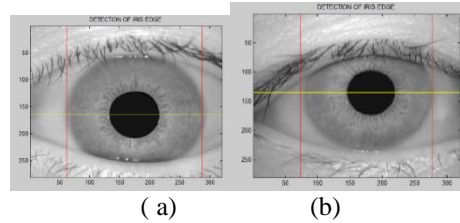


Figure.14 Plotting Lines On Iris And Pupil Boundaries

In the Figure.14.(a) and (b) are the eye images of two different persons where the dimension of images are plotted using the red lines on the outer edge of iris along x-axis and yellow line passes through the centre of pupil along the edges of the iris outer boundary along y-axis. The right and left edges are determined by the change in intensity value of fixed window size. The radius of iris and pupil are defined using the equation (16).

$$\text{Radius} = (\text{right edge} - \text{left edge}) / 2 \quad (16)$$

where right edge is edge on right side of pupil and iris along x-axis, left edge is edge on left side of pupil and iris along x-axis, rx is the radius along x-axis resp.

Table.1. and Table.2. Show the computed values of coordinate along right and left edges of pupil and iris along x-axis and radius of inner and outer boundary. In this experiment we tested the samples of the single person with 7 different orientation angles and computed the iris and pupil dimensions which are tabulated in the result table of Table.1 and Table.2 respectively. It is observed from the above Table.1. and Table.2 that there is very small variation in the radius of all iris images with 7 different orientations corresponding to a single person.

Table.1. Computed Iris Dimensions Of a Person With 7 Different Orientations

Image of person_1	Right edge of iris	Left edge of iris	Radius of iris
Person_1:Sample 1	274	74	100
Person_1:Sample 2	271	71	100
Person_1:Sample 3	270	65	103
Person_1:Sample 4	280	86	97
Person_1:Sample 5	288	88	100
Person_1:Sample 6	276	74	101
Person_1:Sample 7	248	48	100

Table.2. Computed Pupil Dimensions of a Person With 7 Different Orientations

Iris Image of person_1	Right edge of pupil	Left edge of pupil	Radius of pupil
Person_1:Sample 1	221	144	38
Person_1:Sample 2	215	132	40
Person_1:Sample 3	214	135	40
Person_1:Sample 4	225	141	42
Person_1:Sample 5	218	138	40
Person_1:Sample 6	221	138	40
Person_1:Sample 7	193	117	37

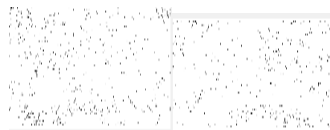
However it seen in Table.3 that, there is a large variation in the iris radius for the sample images of ten different people as indicated by average value (100 to 128.53 pixels) and standard deviation (from 1.13 to 5.77) of iris radius.

Table.3. Computed iris Radius (Minimum, Maximum, Average) of 10 people with 7 orientation of each person

Sample iris image of different Persons	Minimum value of iris radius	Maximum value of iris radius	Average value of iris radius	Standard deviation/Tolerance band
1	98	103	100.29	1.50

2	125	130	128.43	2.37
3	98	110	107.43	4.28
4	100	108	106.86	3.02
5	95	103	99.14	2.48
6	125	128	125.43	1.13
7	106	110	108.43	1.40
8	100	105	102.43	2.15
9	93	98	96.00	2.00
10	100	118	105.57	5.77

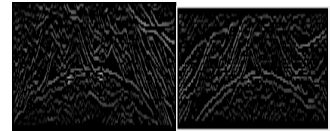
Figure.15. (a) & (b) are the result images obtained after subjecting images in Figure. 13 to the procedure mentioned in the flow chart of Figure.2. This helped to obtain coordinates corresponding to eyelash which are then replaced by the zero value as these are unwanted information. The intermediate results of these operations are shown in figures from Figure.16. to Figure.25. The final output with eliminated eyelashes and eyelids is shown in Figure.25. (a) & (b) respectively for the two iris sample images.



(a) (b)
Figure.15. Gradient Amplitude On The Image Eyelids



(a) (b)
Figure.16. Contrast Enhancement Of The Eyelids



(a) (b)
Figure.17. Non Maxima Suppressed On Eyelids Of The Images



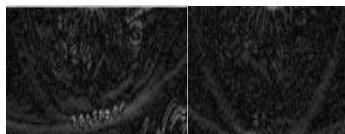
(a) (b)
Figure.18. Hysteresis Thresholding On Eyelids Of The Images



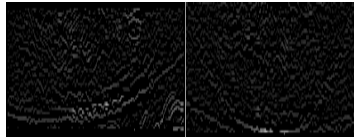
(a) (b)
Figure.19. Detection Of The Top Eyelid Of The Images



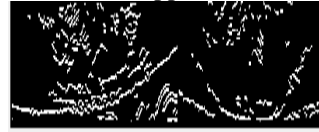
(a) (b)
Figure.20. Gradient Calculation Of The Bottom Eyelids



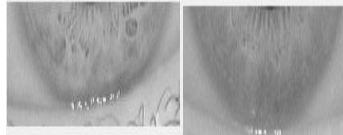
(a) (b)
Figure.21. Contrast Enhancement Of Bottom Eyelids



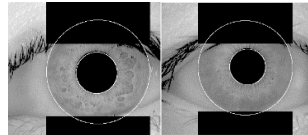
(a) (b)
Figure.22. Nonmaxima Suppression On Bottom Eyelid



(a) (b)
Figure.23. Hysteresis Thresholding On Bottom Eyelids

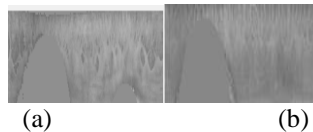


(a) (b)
Figure.24. Detection Of Bottom Eyelids



(a) (b)
Figure.25. Elimination Of Eyelids And Eyelashes

The eliminated Eyelid and eyelashes image obtained in Figure. 25. (a) and (b) is circular in nature, it needs to be represented in rectangular for images in Figure.25. So here the Cartesian to polar conversion is accomplished using Daugman's rubber sheet model described in Section III(C). The images obtained after the conversion in rectangular form called as iris templates which are shown in Figure.26. (a) and (b). Daugman's model removes the redundant iris data and helps in feature extraction which can be further used for iris recognition.



(a) (b)
Figure.26. Normalized Iris Images

Table.4. Computed Pupil Radius (Minimum, Maximum, Average) of 10 people with 7 orientation of each person

Sample iris image of different Persons	Minimum value of Pupil radius	Maximum value of Pupil radius	Average value of Pupil radius	Standard deviation/Tolerance band
1	37.00	42.00	39.57	1.62
2	48.00	53.00	51.29	1.70
3	38.00	43.00	40.86	2.19
4	48.00	52.00	50.00	2.00
5	67.00	75.00	70.71	2.63
6	43.00	48.00	45.14	2.19
7	43.00	51.00	45.71	3.40
8	37.00	40.00	38.71	1.25
9	38.00	43.00	41.29	1.70
10	47.00	52.00	48.71	1.98

Also it seen in Table.4.that there is a large variation in the pupil radius for the sample pupil images of ten different people as indicated by their average value(from 38.71 to 45.72) and standard deviation (from 1.25 to 3.4) of pupil radius. Thus all 756 eye images of 108 people each of size 280x320 pixels are converted to iris templates each of Size 50x250 pixels using the procedure presented in this paper which has useful feature information for classification.

6. CONCLUSION & FUTURE SCOPE

In this paper we have presented the segmentation and normalization method on iris eye images using canny edge detector which used Gaussian filter for edge detection along with Hough transform for circular and linear shape detection. This was followed by application of Daugman's rubber sheet model for normalization process of template formation. This assists for dimensionality reduction and also to accentuate classification accuracy. Classification and identification of iris is a major concern for various bio-inspired applications. So using processed iris images can be used for Iris identification which is one of the future scope

7. ACKNOWLEDGMENT

I would like to express my sincere gratitude towards Prof. Dr. Mrs.V.Jayashree Professor in Electronics Engineering of DKTE Society's Textile & Engineering Institute, Ichalkaranji (An Autonomous Institute) , who has been my supervisor. She has been my philosopher, mentor and guide. She provided me with many helpful suggestions, important advice and constant encouragement in this work.

8. REFERENCES

- [1]. Ghassan Mahmoud Husein Amer, Ahmed Mohmed Abushaala ,“ Edge Detection Methods”,pages 1- 7,DOI:10.1109/WSWAN.2015.7210349, 2015 2nd World symposium on Web Applications and networking.
- [2]. L. Chandrashekar , G.Durga , “ Implementation of Hough transform for image processing application”, IEEE conference publication in International conference on Communication Processing ,2014, DOI: 10.1109/ICCSP.2014.6949962,pp: 843-847.
- [3]. G. J. Daugman, How iris recognition works, IEEE Transactions on CSVT 14(1):21-30 (2004)
- [4]. R.P. Wildes, “Iris recognition an emerging biometric technology”, Proceeding of the IEEE, Vol:85, DOI:10.1109/5.628669, pp:1348-1363.
- [5]. Sanchez-Avila C. and Sanchez-Reillo R. 2002. Iris-based biometric recognition using dyadic wavelet transform. IEEE Aerosp. Electron. Syst. Mag., Vol. 17, pp. 3–6.
- [6]. J.Daugman, “How iris recognition works”, IEEE Transaction on circuit and systems for video technology, vol.14, 2014, DOI:10.1109/TCSVT.2003.818350, pp:21-30.
- [7]. J.Daugman, “New Methods In Iris Recognition”, IEEE Transaction On Systems, Man And Cybernetics, Part B (cybernetics), vol: 37, 2007, DOI: 10.1109/ TSMCB.2007.903540, pp: 1167-1175.
- [8]. [Online]. Available: <http://www.cbsr.ia.ac.cn/IrisDatabase/irisdatabase.php>
- [9]. B.G.Patil.”Human iris pattern recognition using phance components of image”,IEEE Conference On Industrial and Information System(ICIIS),DOI:10.1109/ICIINFS.2009.5429900,PP:10-14